AN UNEQUAL POWER ALLOCATION DESIGNED FOR MIMO SYSTEMS USING CONTENT CHARACTERISTICS

Julien Abot, Clency Perrine, Yannis Pousset & Christian Olivier
University of Poitiers, Department of Signal Image and Communication, XLIM Institute,
CNRS JUR 7252, France

ABSTRACT

This paper presents an Unequal Power Allocation (UPA) strategy for the transmission of a JPEG 2000 Wireless (JPWL) image. To ensure the Quality of Service (QoS), we exploit the channel diversity with a Closed-Loop MIMO scheme. It relies on the Channel State Information (CSI) knowledge at the transmitter side that diagonalizes a MIMO channel into several hierarchical SISO subchannels. In the proposed scheme, the JPWL codestream is divided into hierarchical quality layers passing through the SISO subchannels. According to this strategy, we propose a new content-based precoding algorithm to maximize the visual quality in reception. This algorithm is compared with four other precoders of the literature such as Water Filing (WF), Minimum Mean Square Error (MMSE), Minimum Bit Error Rate (MBER) and Equal-d_{min} (E-d_{min}). Indeed, we show that power allocation of these precoders is not suitable to ensure QoS of a hierarchical content. We compare precoders' performances on a statistical channel and a realistic time-varying MIMO channel provided by a 3D-ray tracer propagation model. Results show that our proposed approach improves the visual quality. We also present a study highlighting the good robustness of the algorithm to channel estimation errors.

Keywords: *Image transmission, Wireless JPEG 2000, Quality of Service, realistic MIMO channel, Unequal Power Allocation.*

1. INTRODUCTION

During the last decade, wireless communications are widely developed. The emergence of several new wireless communications standards such as 4G, Long Term Evolution (LTE) or Wifi has increased the potential of wireless networks. Image transmissions are one of the many possibilities allowed by these networks. However, the well-known constraints of the transmission environment such as limited bandwidth, frequency fading and Doppler effect can affect the QoS required by end users.

Considering the physical layer, Multiple Input Multiple Output (MIMO) with Orthogonal Frequency-Division Multiplexing (OFDM) technologies have shown their efficiency to improve the QoS using the maximum diversity of wireless channel [1]. Considering the application layer, the proposed strategies in the literature are become more sophisticated in order to adapt parameter values to the transmitted content. An important point is that compressed images are generally hierarchical in content, which results in the unequal importance of data. Because of this, Unequal Error Protection (UEP) strategies [2] [3] [4] have demonstrated an undeniable interest in image transmission. In a similar way, the power weighting during a transmission has been notable to enhance the QoS in a content transmission, as exemplified in [5] [6]. It should be noted that the design of MIMO systems is particularly adapted for UPA strategies. For example, the authors in [7] proposed an UPA scheme for the transmission of JPEG compressed images over MIMO systems. The image is divided into qualitatively different streams, these streams being simultaneously transmitted from different antennae of varying power using spatial multiplexing. The aim of the model is to minimize the overall distortion of the received image. Results for low channel SNRs show quality gains of around 14 dB in terms of PSNR, in a comparison with the EPA scheme.

There are two types of MIMO techniques based on whether or not one knows Channel State Information (CSI) at the transmitter side. Open-loop MIMO schemes only consider the CSI knowledge from the point of view of the receiver side with specific codes like Space-Time Block Code [8]. Conversely, Closed-loop MIMO schemes take into account the CSI knowledge from the point of view of both receiver and transmitter side to achieve better performances than open-loop MIMO scheme [9]. This feedback information allows decomposing the MIMO channel into independent and hierarchical SISO subchannels [10], and then allows UPA strategies by algorithms called precoders. These algorithms are generally based on optimization problem under constraints of a specific criterion, such like the channel capacity (WF precoder [11]), the Minimum Mean Square Error (MMSE precoder [11]), the Minimum Bit Error Rate (MBER precoder [12]) or the constellation minimum distance denoted d_{min} (E-d_{min} [13]). However, these techniques do not jointly take into account the content and the systems parameters (subchannel SNRs, power, modulation and channel coding), which have an effect on the rate-distortion trade-off [14].

So, this paper presents the following contributions. We propose a new Closed-Loop MIMO scheme that includes a CSI feedback from the receiver to the transmitter, maximizing the visual quality in reception. It is based on a successive power allocation on the SISO subchannels with QoS constraint on each of them. This QoS constraint is defined by a target Bit Error Rate (BER). We use Wireless JPEG 2000 (JPWL) [15], which is the Part 11 of JPEG 2000 standard. It standardizes tools and methods to achieve the efficient transmission of JPEG 2000 images over an error-prone wireless network. In addition, the JPEG 2000 core coding can divide an image into hierarchical quality layers that is particularly adapted to the transmission on a MIMO channel decomposed into SISO subchannels. A robust JPWL decoder [16] is also used to overcome residual errors. The proposed precoding solution is compared to four well-known other precoder designs (WF, MMSE, MBER and E-d_{min}). In addition, we show that not taking into account the content in the transmission of a hierarchical image decreases the visual quality in reception. To do this, we study the algorithms performances in two cases. Firstly, we compare precoders on a statistical channel with a pseudo-random sequence and without channel coding. Secondly, we study the effect of precoding solutions on the transmission of a JPWL image over a realistic time-varying MIMO channel provided by a 3D-ray tracer propagation model [17]. At last, we show the impact of the CSI error estimation on the received images quality. Indeed, the CSI errors estimations errors are a major issue for a precoded MIMO system.

The paper is organized as follow. Section II describes the global scheme and presents the proposed UPA algorithm. Section III presents the simulation results. Finally, we finish by a conclusion.

2. CONTENT-BASED PRECODING SOLUTION

Figure 1 illustrates the transmission strategy. The main objective is to maximize the visual quality of a JPWL image at the receiver side. The robustness of the scheme is strengthened by matching the JPWL quality layers hierarchy and the SISO subchannel hierarchy this giving a content-based allocation. The visual quality is ensured by an UPA algorithm, which connects the variables of the transmission chain (SNR of each SISO subchannel (CSI), the modulation orders and the correction capability of the used Error Correcting Codes (ECC)).

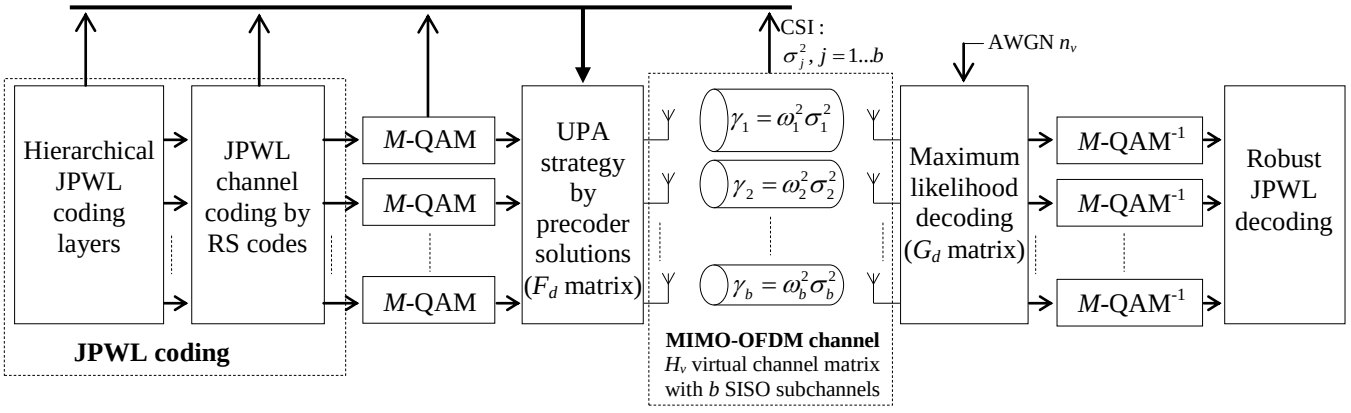

Figure 1. Synopsis of the global scheme

2.1. Precoding on a MIMO Channel

A precoder solution is used in order to decompose the MIMO channel into several uncorrelated SISO subchannels. Precoder designs allow a high flexibility in power allocation with respect to the SISO subchannels. The next step is to define a MIMO system with n_T transmitters and n_R receiver antennae ie. an ($n_T \times n_R$) MIMO system with $b = \min(n_R; n_T)$. The system equation of the MIMO system using precoder designs is given as:

$$y = GHFx + Gn \quad (1)$$

where x and y are the ($b \times 1$) transmitted and received symbol vectors, respectively. H is the ($n_R \times n_T$) MIMO channel matrix, F is the ($n_T \times b$) linear precoder matrix. G is the ($b \times n_R$) linear decoder matrix and n is the ($n_R \times 1$) zero-mean additive noise vector. The common step for all linear precoders is called the virtual transformation. This operation uses the singular value decomposition method to decompose a MIMO channel into uncorrelated SISO

subchannels. After applying the virtual transformation, the diagonal MIMO channel is obtained and is expressed as follows:

$$y = G_d H_v F_d x + G_d n_v \tag{2}$$

where $H_v = G_v H F_v$ is the eigen-channel matrix including the eigen-values $\sigma_j^2, j = 1...b$, G_v and F_v are unitary matrices and $n_v = G_v n$ is the transformed white additive noise vector with covariance matrix $R_{n_v} = I_b$, I_b is b size identity matrix. The F_d and G_d are, respectively, the precoding and decoding matrices. In this paper, the Maximum Likelihood (ML) criterion is used to detect the received symbols. Without any loss of generality, the decoding matrix G_d is viewed as a unitary matrix. The diagonal precoder solutions are therefore defined only by the diagonal precoding matrix F_d. One of the purposes of this work is to compute the precoding parameters (coefficients of F_d diagonal matrix), denoted $\omega_j^2, j = 1...L$, in accordance with the other system variables (CSI, modulation order and ECC correction capability), under the constraint of the total transmitted power (E_T): $\sum_{j=1}^{L} \omega_j^2 \le E_T$. This allows the computation of the SNR after a precoding step such as:

$$\gamma_j = \omega_j^2 \sigma_j^2 \text{ with } j = 1...L \tag{3}$$

where $\gamma_j, j = 1...L,$ is the Signal to Noise Ratio on subchannel j weighted by the precoding coefficient $\omega_j^2, j = 1...L$. The precoding coefficients computed for the L used SISO subchannels and provide an insignificant BER in reception. Finally, the quality of the ($n_T \times n_R$) MIMO channel is assessed by its total gain σ, computed as follows:

$$\sigma = \sqrt{\sum_{j=1}^{b} \sigma_j^2} \tag{4}$$

2.2. Unequal Power Allocation Algorithm

The current investigation proposes a power allocation model under a BER constraint. This algorithm connects the parameters of the transmission chain i.e. the SNR value of each SISO subchannel, the modulation orders and the ECC correction capability. These parameters are jointly considered to compute the precoding coefficients $\omega_j^2, j = 1...L$. It is assumed that the noise on the SISO subchannels is Gaussian [10]. Thus, the binary error probability $P_{eb,j}$ on subchannel j for the M_j-QAM modulation can be formulated using the following expression [18]:

$$P_{eb,j} = \frac{2\left(\sqrt{M_j} - 1\right)}{\sqrt{M_j} \log_2 M_j} erfc\left(\sqrt{\frac{3\gamma_j}{2(M_j - 1)}}\right) \tag{5}$$

The aim of the model is to formulate the precoding coefficient ω_j^2 on a subchannel j and thus to provide a target BER denoted BER_{Tj}. Accordingly, $P_{eb,j}$ is identified with BER_{Tj} under asymptotic assumption. This leads to:

$$BER_{T,j} = \frac{2\left(\sqrt{M_j} - 1\right)}{\sqrt{M_j} \log_2 M_j} erfc\left(\sqrt{\frac{3\omega_j^2 \sigma_j^2}{2(M_j - 1)}}\right) \tag{6}$$

The precoding coefficient ω_j^2 is derived from (6) to provide $BER_{T,j}$ this being a function of the Eigen value σ_j^2 of the subchannel j and of the order of the QAM modulation M_j. The following equation is generated:

$$\omega_j^2 = \frac{2(M_j - 1)}{3\sigma_j^2}\left[erf^{-1}\left(1 - \frac{BER_{T,j}\sqrt{M_j}\log_2 M_j}{2\left(\sqrt{M_j} - 1\right)}\right)\right]^2 \tag{7}$$

According to (7), we can compute the needed power to reach $BER_{T,j}$ for a given SNR and modulation order on the subchannel *j*. We can note that for a lower target BER with the same modulation, the algorithm will provide more power (higher precoding coefficient). Moreover, if the spectral efficiency of the modulation is increased so as to reach the same $BER_{T,j}$, the algorithm must also provide more power.

2.3. Using RS Codes Rate for $BER_{T,j}$ Definition

At this demonstration step, the proposed algorithm does not yet consider the ECC correction capability. Thus Reed Solomon (RS) codes are considered because they are already implemented in the JPWL standard. An RS code is defined by the parameters using the symbols *K* and *N*, which are connected to the number of bits before and after channel coding respectively. s_j is the number of bits per symbol on the subchannel *j* such as $s_j = \log_2(M_j)$ with *j* = 1...*L*. So, the binary error probability $P_{RS,j}$ after channel decoding by a given RS(N_j,K_j) code on s_j-bits symbols, is [18]:

$$P_{RS,j} = \frac{1}{s_j} \sum_{i=t_j+1}^{N_j} \frac{i}{N_j} \binom{N_j}{i} P_{S,j}{}^{i} \left(1 - P_{S,j}\right)^{N_j - i} \tag{8}$$

where $P_{S,j} = s_j P_{eb,j}$ is the symbol error probability on a s_j-bits symbol and $t_j = \lfloor (N_j - K_j)/2 \rfloor$ is the correction capability for the given RS(N_j,K_j) code. According to (5) and (6), $P_{eb,j}$ depends on the precoding coefficient ω_j^2 and is identified with $BER_{T,j}$. Thus:

$$P_{S,j} = s_j P_{eb,j} = s_j BER_{T,j} \tag{9}$$

Let us define B_j, the target BER after channel decoding on a subchannel *j*, such that $P_{RS,j} \le B_j$, then [see (8)]:

$$\frac{1}{s_j} \sum_{i=t_j+1}^{N_j} \frac{i}{N_j} \binom{N_j}{i} \left(s_j BER_{T,j}\right)^{i} \left(1 - s_j BER_{T,j}\right)^{N_j - i} \le B_j \tag{10}$$

The B_j parameter is thus the acceptable BER on the j^{th} quality layer before source decoding. This value must be determined according to the content. As example, in the case of a variable-length coding, where a single error may desynchronize the bitstream, one will choose sufficiently low value for B_j corresponding to a quasi error free transmission. If the desynchronizations are not a problem (fixed length coding), we can set the B_j parameter depending on the type of data. As example, the hierarchy existing between the wavelet subbands could be used (or between DC and AC coefficients of DCT-based coder). Thus, this algorithm is flexible and can adapt to the characteristics of the transmitted content.

An approximation of the $BER_{T,j}$ values is computed using an iterative algorithm. This allows to reach the B_j boundary according to a given RS(N_j,K_j) code. The decrease of the B_j boundary leads to a decrease in the $BER_{T,j}$ parameter and an increase in the precoding coefficient. Thus, the proposed UPA solution called Content-Based Precoder (CBP), allowing high flexibility in the power allocation process, can be jointly adapted to the channel status and the magnitude of the JPWL quality layer transmitted over the *b* SISO subchannels. To finely adjust the power allocation, the ECC correction capability and the order of modulation are taken into account.

3. SIMULATION RESULTS

In this section, the proposed CBP algorithm is compared with WF, MMSE, MBER and E-d_{min}. First, we study the performances of these algorithms on a statistical channel without content consideration (pseudo-random sequence), only in terms of BER. Second, we compare the results of a JPWL image transmission over a realistic channel in order to assess the impact of the algorithm when transmitting a hierarchical content, evaluated according to the PSNR metric. We then examine the impact of a Gaussian error model on the estimated CSI for the performances of the strategy.

3.1. Simulation on Statistical Channel

3.1.1. System Description

We use a 4×4 MIMO system that leads to consider 4 SISO subchannels with 4-QAM on each of them. Symbols resulting of the 4-QAM constellation are randomly generated. For each symbols vector, we generate a new Rayleigh

channel matrix H and a new noise correlation matrix $R = TT^*$ where T^* is the hermitian matrix of T. H and T elements are complex Gaussian random variables, independent and identically distributed (i.i.d.), centered with unit variance. R matrices are normalized according to the SNR. For each SNR level, we transmit 10^5 symbols vectors without ECC. For these tests, $BER_{T,j}$ parameter is set to 10^{-9} for $j = 1 \ldots L$, this corresponding to a quasi-error free transmission.

3.1.2. Results on a Statistical Channel

The figure below presents the BER variation on the MIMO channel according to the power allocation strategy (figure 2). We consider the global BER resulting from the average BER of each SISO subchannel, which is a classic criterion for the comparison of precoders in the literature. To properly analyze this figure, we point out that CBP, WF, MMSE and MBER are diagonal precoders (with diagonal F_d matrix) while E-d_{min} is a non-diagonal precoder (with non-diagonal F_d matrix).

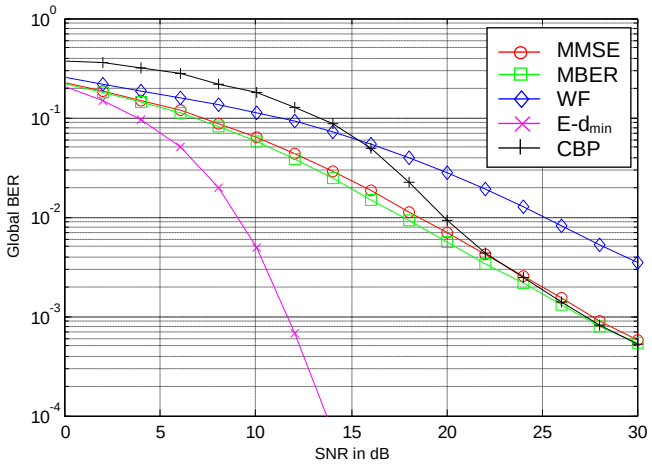

Figure 2. Global BER on the MIMO channel

Considering the global BER on the MIMO channel, other precoders provide better results than CBP solution until SNR of 15dB for WF and around 22dB for MMSE and MBER. For higher SNR levels, results are widely better than WF, while they are much closer with MMSE and MBER. This explains by the optimization used by the other precoders. The optimization of a specific criterion on the full set of subchannels leads to reduce the BER on each of them. Inversely, the most disadvantaged subchannels are voluntarily unused by CBP precoder if they do not respect QoS constraint. Thus, the BER on unused subchannel becomes very high (equal to 0.5) making global BER higher than global BER provided by other precoders. E-d_{min} performances are widely higher than the others precoders because E-d_{min} is a non-diagonal precoder which gives additional degrees of freedom. This precoder can thus vary the transmission power and the geometry of the constellation which allows achieving a better BER, especially on the fourth subchannel. However, a hierarchical content has special characteristics. Indeed, during the transmission, to decode data (packet or quality layer) with a given index n, it is necessary to correctly decode all previous data (with indices n-1, n-2, ..., 1). As a consequence, QoS evaluation during the transmission of hierarchical content need to consider the precoder behavior on each SISO subchannel as we can see on the figure 3.

This figure presents the BER variations on each SISO subchannel according to the precoding solutions. The CBP solution is designed to maximize the visual quality of an image in reception by a better respect regarding the image hierarchy. Unlike the other power allocation strategies, the CBP solution makes sure the correct transmission (defined by $BER_{T,j}$) of the base quality layer on the first subchannel, when the channel conditions are bad (SNR < 5dB). CBP successively allocates power on the other subchannels (corresponding to the additional layers) according to the improvement of the channel conditions. This successive distribution of power jointly considering the subchannel SNRs and the modulation order and under QoS constraint is an enhancement factor of visual quality in reception. On the contrary, the other precoders allocate power on the subchannels independently both of the content and the system settings. As a consequence, in the case of a pseudo-random sequence, the other precoder performances may be overall better than our proposed algorithm especially for lower SNR. However, these precoders make no guarantee about the QoS for a hierarchical content transmission.

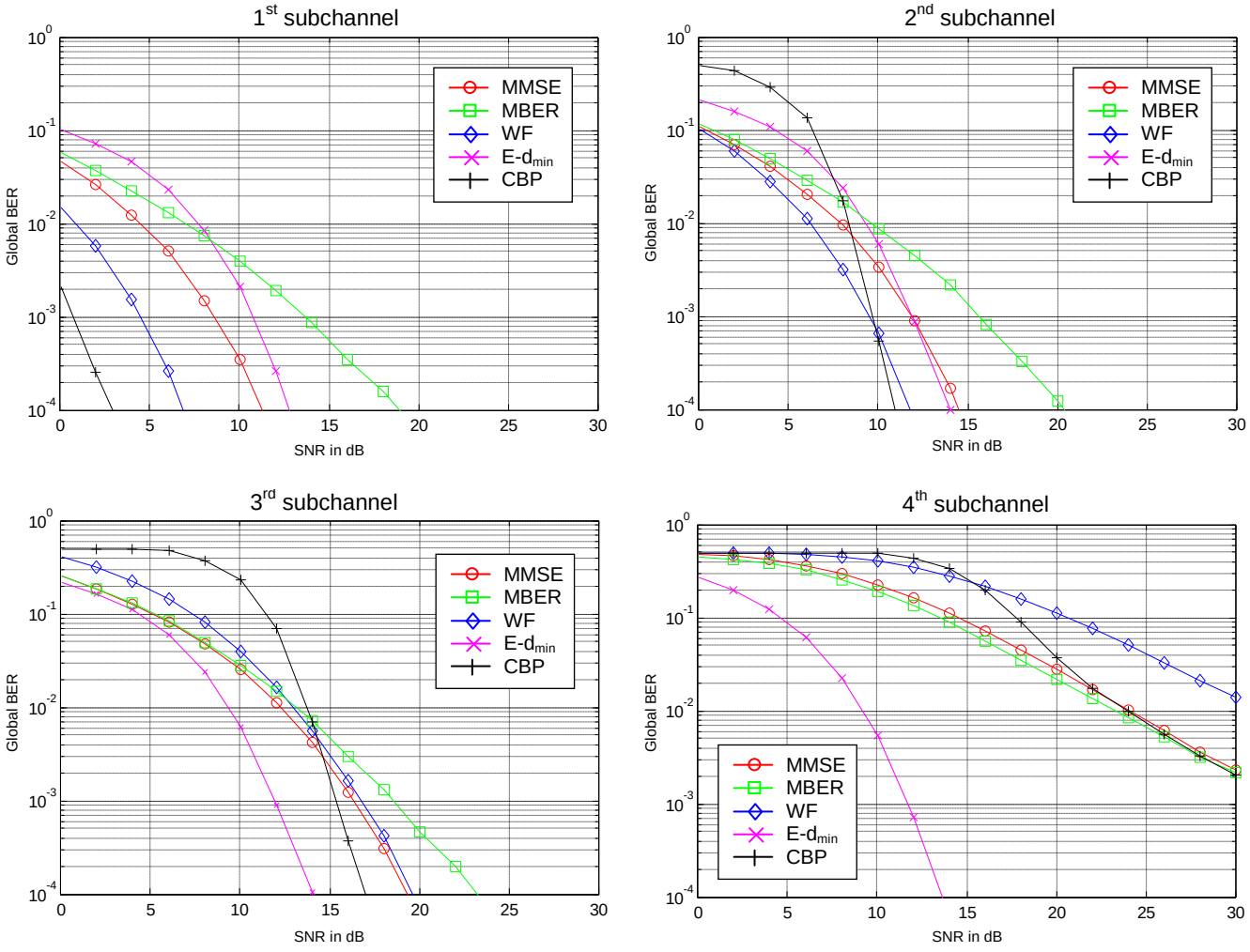

Figure 3. BER variations on each SISO subchannel

3.2. Simulation on Realistic Channel

3.2.1. System Description

The transmission chain includes parameters of *IEEE802.11n* standard [19]. However, we do not use ECC provided by this standard but we use the RS codes provided by the JPWL standard. We consider 4-QAM and the OFDM modulation included in the *IEEE802.11n* standard with OFDM symbol period equals to 4µs. The CSI is known at both the transmitter and receiver sides. It provides σ_j^2 with j = 1…4. We are not under perfect CSI knowledge assumption. An imperfect CSI knowledge is taken into account at both the transmitter and receiver side. The CSI is only updated at regular intervals that generate errors between two estimations caused by channel variations. A new channel estimation is performed every 20 OFDM symbols in order to minimize the channel variations and may limit the Doppler effect.

3.2.2. Wireless JPEG 2000 features

Figure 4 represents the JPWL codestream organization. The transmitted image is coded by JPWL into 4 quality layers. Each layer passes through a SISO subchannel and contains useful and Error Protection Bloc (EPB) data. Main header and tile-part header are allocated on the first subchannel. Each of layer is coded at 0.125bpp including EPB data and headers for the first layer. JPWL allows decomposing an image into different parts (called tiles) to reduce the coding complexity. However, we consider only one tile to code the image. To overcome transmission

errors, we use the tools of JPWL [15] such as SOP (Start Of Packet) and EPH (End of Packet Header) resynchronization markers. Main header protection and tile-part header protection predefined by the JPWL standard are also included. In order to test the presented transmission strategy, two cases for simulation are considered such as without ECC on useful data and then RS(37,32) codes on useful data. We choose the smallest RS code of the JPWL standard in Equal Error Protection strategy, to highlight the robustness of the global scheme. However, an UEP strategy can easily be implemented but this is not the purpose of this paper (this issue is discussed in [14]). We use "Caps" and "Monarch" colour images (selected for their content diversity) with resolution of 768×512 pixels for simulations. We consider a received layer is quasi-error free if the BER is limited to 10^{-9}, so $B_j = 10^{-9}$ for $j = 1 \ldots L$. According to (10), for $B_j = 10^{-9}$ without ECC, we consider $BER_{T,j} = 10^{-9}$ and by using RS(37,32) codes, we consider $BER_{T,j} = 2.92 \times 10^{-5}$.

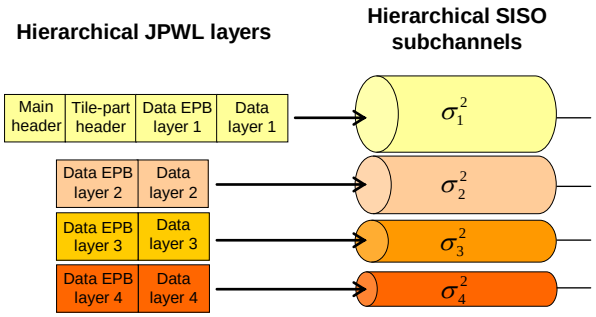

Figure 4. JPWL quality layers and EPB data repartition on SISO subchannels

3.2.3. Realistic Error-Prone Environment

A realistic time-varying MIMO channel in a suburban environment is used for simulations (figure 5).

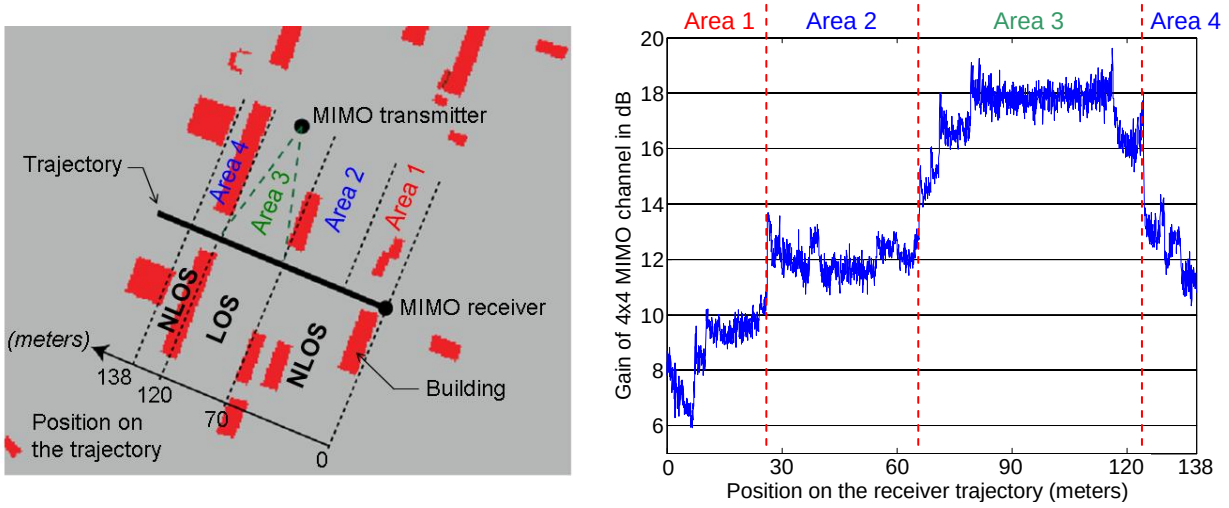

(a) Topology of the transmission scene

(b) Gain variation of the MIMO channel

Figure 5. Realistic transmission environment

The channel complex impulse responses used for simulation takes into account multipath and mobility in a realistic way. These are provided by a 3D-ray tracer channel simulator [17]. In figure 5(a) the buildings are in red. The MIMO transmitter is fixed and the MIMO receiver moves throughout a distance of 138m at a speed of 5 m/s. In this configuration, MIMO receiver goes through the scene alternating NLOS (Non Line Of Sight) and LOS conditions. Thus MIMO receiver successively meets bad (NLOS in area 1), average (NLOS in areas 2 and 4) or good conditions (LOS in area 3). The variation of the total MIMO channel gain σ is presented in figure 5(b). σ is defined by (4).

3.2.4. Results on Realistic Channel

Figure 6 presents the variation of the PSNR according to the position on the receiver trajectory. During the simulation, images are continually transmitted through 2300 simulation steps that lead to receive 2300 images. Two cases are considered: without ECC on the useful data (figure 6(a)) and with RS(37,32) codes on the useful data (figure 6(b)). Only the curves characterizing the "Caps" image are represented. Curves for the ''Monarch'' images are not represented because they manifest similar behavior to the curves for the ''Caps'' image. However, results for all images are represented in tables 1 ("Caps") and 2 ("Monarch") in terms of mean PSNR regarding the channel conditions.

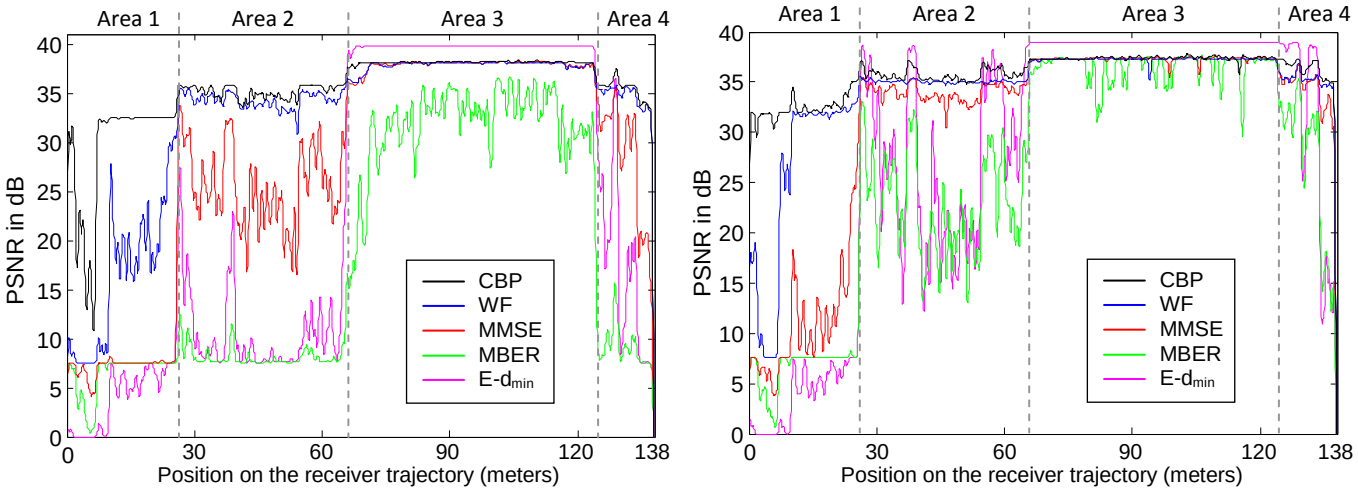

(a) No ECC on useful data

(b) RS(37,32) codes on useful data

Figure 6. PSNR variation according to the precoders for "Caps" image

In the case of a hierarchical image transmission on a realistic channel, we note that performances of the other precoders are generally lower than those presented by CBP solution, especially in bad conditions (fig. 6, area 1). There are two main explanations. First, other precoders do not take into account some parameters having an effect on the rate-distortion trade-off. Consequently, these precoding solutions do not modify their power allocation policy whatever the correction capability of an ECC or the modulation sensitivity. Second, other precoders optimize specific parameters (channel capacity, MSE, BER, d_{min}) without taking into account the hierarchical content. The problem is considering on the full set of the subchannels without QoS constraint on each of them. The result is the possibility to not allocate enough power to make a useful subchannel. In the case of a hierarchical content, a failure in the decoding of the quality layer of index *n*, prevents the decoding of the layers with index higher than *n*. In practical terms, this explains the lower performances of other precoders in comparison with the CBP solution, in particular in the areas where the channel is disturbed.

E-d_{min} precoder presents a particular behavior. Remind that it is the only non-diagonal precoder that offers additional degrees of freedom compared to the diagonal precoder. In this case, it allows obtaining a BER roughly equivalent to all SISO subchannels (fig. 3). Therefore, either the BER on the SISO subchannels are too high to achieve an acceptable result (mean PSNR < 20dB, table 1 and 2), or the BER is low enough to decode all quality layers in good conditions (table 1 and 2), while the diagonal precoders can decode three quality layers at best.

Table 1. Average performances in terms of PSNR (dB) for "Caps" image

CHANNEL CONDITIONS	**BAD** Area 1 - NLOS		**AVERAGE** Areas 2 and 4 - NLOS		**GOOD** Area 3 - LOS	
CHANNEL CODING ON USEFUL DATA	*no ECC*	*RS(37,32)*	*no ECC*	*RS(37,32)*	*no ECC*	*RS(37,32)*
WF	16.38	25.65	34.41	35.11	37.86	37.29
MMSE	7.31	11.05	26.23	34.09	37.87	37.31
MBER	6.50	6.68	8.41	23.85	31.59	36.54
E-d_{min}	3.90	3.73	12.47	27.93	**39.73**	**38.93**
CBP	**29.40**	**32.45**	**35.20**	**35.89**	38.12	37.39

Table 2. Average performances in terms of PSNR (dB) for "Monarch" image

CHANNEL CONDITIONS	**BAD** Area 1 - NLOS		**AVERAGE** Areas 2 and 4 - NLOS		**GOOD** Area 3 - LOS	
CHANNEL CODING ON USEFUL DATA	*no ECC*	*RS(37,32)*	*no ECC*	*RS(37,32)*	*no ECC*	*RS(37,32)*
WF	14.54	22.26	31.23	32.16	35.37	34.70
MMSE	6.66	9.34	22.70	30.93	35.28	34.72
MBER	5.91	6.06	7.67	20.49	28.38	33.99
E-d_{min}	3.42	3.47	11.11	25.36	**37.52**	**36.70**
CBP	**26.17**	**28.78**	**32.29**	**33.07**	35.60	34.80

The proposed solution takes into account modulation and channel coding to provide power only for the subchannels that are considered exploitable in reception under QoS constraints. It can be noted that CBP is the only precoder to provide a good QoS in the lack of channel coding on the useful data (fig. 6 (a)). It also takes into account the correction capability of the RS code (fig. 6(b)) to decrease the value of the target BER which leads to decrease the allocated power on a SISO subchannel. Accordingly, CBP can transmit more quality layer with respect to the configuration without channel coding, thereby increasing the QoS.

3.2.5. Visual results

Figures 7 and 8 show representative visual results obtained when transmission conditions are bad (Fig. 7) or average (Fig. 8).

CBP **WF** **MMSE, MBER, E-d_{min}**

(a) PSNR = 32,45dB (b) PSNR = 24,01dB (c) PSNR = 7,53dB

Figure 7. Visual results for "Caps" image in bad channel conditions (15 meters) without channel coding on useful data

When channel conditions are bad (area 1 in fig. 5(b)), CBP only allocates power on the first subchannel, to ensure the correct decoding of the base quality layer without distortion related to the transmission errors. WF allocates power for the transmission of two quality layers. Then, there is then a lack of power on the first SISO subchannel

(which carries the base quality layer), resulting in visual distortions. MMSE, MBER and E-d_{min} do not allocate enough power on the first subchannel to decode the base layer. This misapprehension of a hierarchical content characteristics leads to a waste of power (allocation to transmit unusable data).

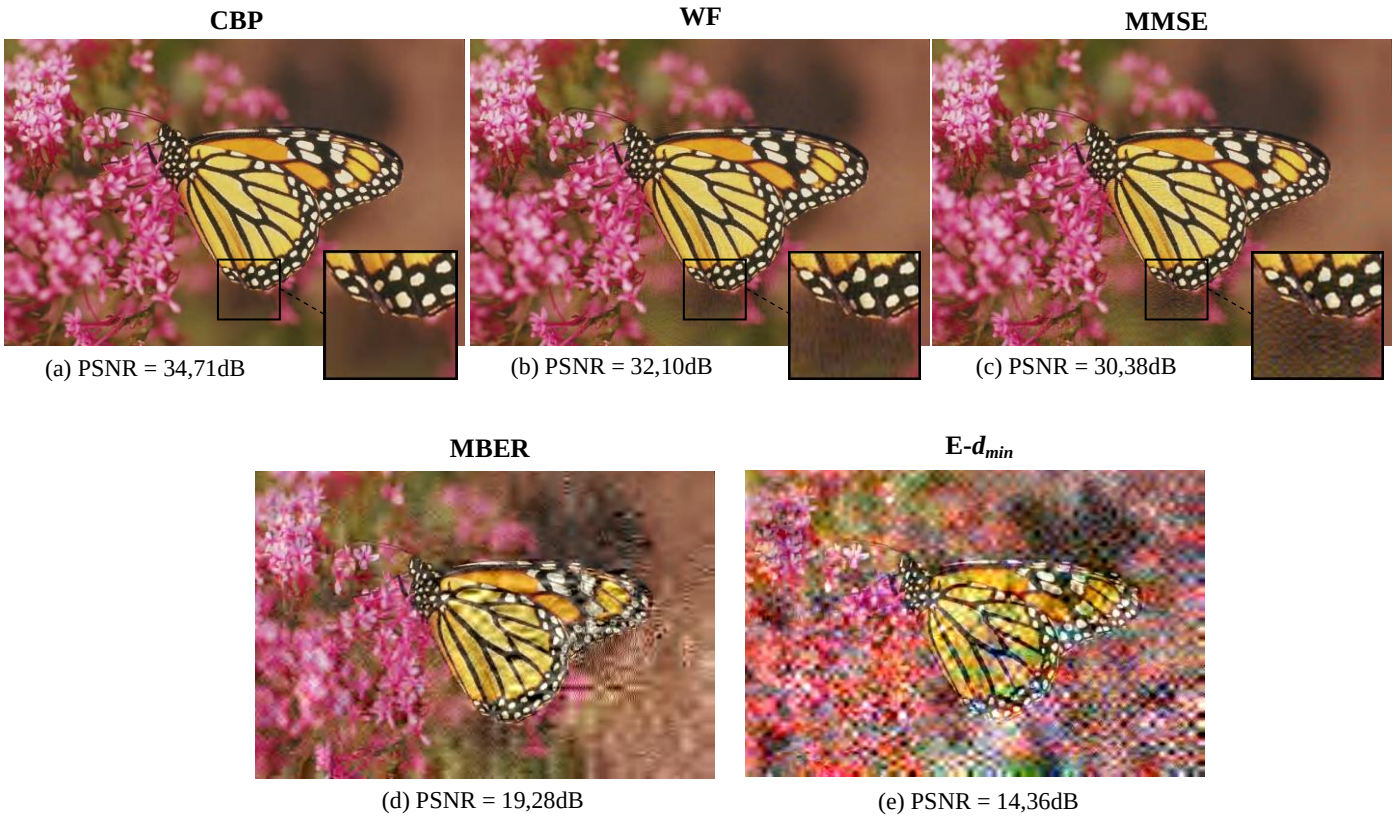

Figure 8. Visual results for "Monarch" image in average channel conditions (135 meters) with RS code on useful data and zoom to compare better results

When channel conditions become average (areas 2 and 4 in fig. 5(b)), we find that MBER and E-d_{min} still have difficulty for decoding the base quality layer. Only CBP, WF and MMSE precoders provide an acceptable result. However, if we look in detail, only CBP presents a version of the image without distortion due to transmission errors. Once again, this is explained by the fact that CBP sends few layers but it ensures that the layers transmitted can be usable, while this is not the case with other precoders of literature.

3.2.6. Impact of Estimation Errors on CSI

The knowledge of the CSI is a major issue in the field of telecommunications. Indeed, it can be difficult to consider a perfect knowledge of the instantaneous CSI characterizing the MIMO-OFDM channel. This explains why we did not assume a perfect CSI knowledge in our works, but only a "perfect" CSI updating at regular intervals (see §3.2.1).

However, the impact of CSI estimation errors during the update are explored in this section. We use a Gaussian error model on the CSI estimation which is frequently used in the literature [13]. In figure 9, we investigate the impact of imperfect channel knowledge at both transmitter and receiver side on the BER performance. In general, the estimated channel matrix H_{est} is modelled as $H_{est} = H + H_{err}$ where H_{err} represents the channel estimation error. A more complete description of H_{est} can be found in [20] for two different methods of channel estimation. It is assumed in this paper that entries of H_{err}, independent of H, are composed of complex Gaussian i.i.d random variables with mean zero and variance σ_{err}^2. Higher the SNR is, smaller σ_{err}^2 is; in our simulation we set $\sigma_{err}^2 = \beta\sigma^2$ with $\beta = 0.25$.

We use the most robust configuration previously used, including RS(37,32) codes on useful data. Figure 9 shows the variation of the PSNR for the "Caps" image without CSI errors (figure 9(a)) and with CSI errors (figure 9(b)). We

only represent the results of the "Caps" image because the conclusions are exactly the same for "Monarch". Table 3 presents a comparison of mean PSNR regarding the channel conditions obtained with and without error model. For these tests, we consider two configurations of the parameter B_j (B_j = 10^{-9} and 10^{-12}) with j = 1...L for the CBP precoder.

As we can see in Figure 9, all precoders are penalized by lower PSNR. Considering the precoders of the literature, we note that they are ineffective (mean PSNR < 10dB) in bad transmission conditions (area 1). When channel conditions become average (areas 2 and 4), only the WF precoder provides QoS (mean PSNR = 33.21dB) with a moderate loss on the mean PSNR of 1.9dB. In good transmission conditions (area 3), the precoders of the literature are weakly affected by estimation errors in the CSI (the mean PSNR loss of less than 1dB), except for MBER which loses approximately 7dB on the mean PSNR.

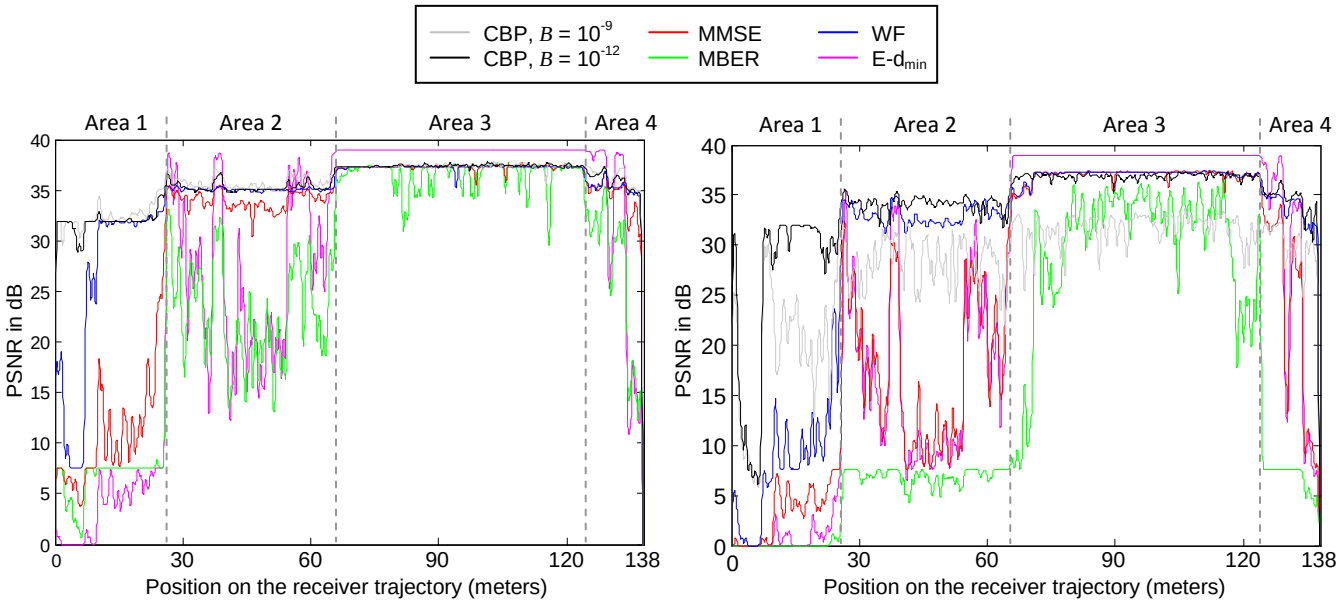

(a) without CSI errors (b) with CSI errors

Figure 9. Impact of estimation errors on CSI

Table 3. Impact of estimation errors on the CSI in terms of mean PSNR (dB) for "Caps" image

CHANNEL CONDITIONS	**BAD** Area 1 - NLOS		**AVERAGE** Areas 2 and 4 - NLOS		**GOOD** Area 3 - LOS	
CSI ESTIMATION ERROR	*Without*	*With*	*Without*	*With*	*Without*	*With*
WF	25.65	8.50	35.11	33.21	37.29	37.08
MMSE	11.05	3.24	34.09	19.45	37.31	37.00
MBER	6.68	0.10	23.85	6.92	36.54	29.67
E-d_{min}	3.73	0.98	27.93	19.65	**38.93**	**38.93**
CBP avec B = 10^{-9}	**32.45**	19.55	**35.89**	28.87	37.39	31.71
CBP avec B = 10^{-12}	31.97	**26.15**	35.48	**34.25**	37.40	36.88

We can see that CBP, defined in its previous configuration (B_j = 10^{-9}), is most strongly affected by estimation errors in the CSI. This explains by the target BER that is determined for ideal transmission assumptions including a correct estimate of the CSI. The evaluation of the required power for a subchannel from an erroneous channel matrix leads to a greater received BER than the target BER. Therefore, the RS(37,32) code must correct too many errors regarding to its correction capability. This result occurs in a large number of cases where there are too many uncorrected errors on the base quality layer, which increases the number of cases of non-decoded pictures. Thus, the error estimation of the CSI leads to the largest losses in terms of mean PSNR (12.9dB, 7.02dB and 5.68dB in transmission conditions respectively bad, average and good) among compared precoders.

However, we find that we can significantly reduce the impact of error estimation on CSI strengthening the constraint on the BER in reception. In our example, we set the B_j parameter equal to 10^{-12} for $j = 1 \ldots L$, thereby providing the best overall QoS among the compared precoders. This parameter is specific to CBP and it has no equivalent in other precoders that can not adapt to CSI error estimation assumptions. Increasing the B_j parameter leads to increase the allocated power on a SISO subchannel (to achieve a lower target BER). Therefore, it may happen there is a lack of power to efficiently use a subchannel and to transmit additional enhancement layer. Increasing the target BER has mainly an impact when the channel conditions are bad (around 0.5dB) or average (around 0.4dB). However, this strategy can efficiently reduce the impact of estimation errors on CSI.

4. CONCLUSION

In this paper, we proposed a new content-based precoding solution for the transmission of a JPWL image over MIMO channel decomposing into SISO subchannels. It relies on an allocation regarding source and channel hierarchy to improve the QoS. The proposed UPA algorithm takes into account transmission parameters affecting rate-distortion trade-off such as order of modulation and correction capacity of RS codes, with QoS constraint on each SISO subchannel. We have shown that the overall BER (which is a usual criterion for comparing precoders) is not a relevant criterion for assessing the performance of precoding strategies for image transmissions. In addition, we show that our solution (CBP precoder) provides a better QoS than other precoders of the literature based on optimization of a specific parameter (channel capacity, MSE, BER or d_{min}). Furthermore, this evaluation was carried out in realistic conditions provided by 3D-ray tracer propagation model. We also show the good robustness of the strategy to estimation errors in CSI which represents a major issue for precoded MIMO system. In particular, we have shown the great flexibility of the CBP precoder allows a good adaptation to CSI error assumptions, by strengthening the QoS constraints on each SISO sub-channels. The proposed work is not limited to the JPWL content. It may be expanded to other hierarchical content like video.

5. ACKNOWLEDGEMENTS

This work has received support from the French National Research Agency through the CAIMAN project, ANR-08-TO-002. The authors would like to thank Didier Nicholson and Cyril Bergeron from THALES Communications.

6. REFERENCES

[1] H. Sampath, S. Talwar, J. Tellado, V. Erceg, "A Fourth-Generation MIMO-OFDM Broadband Wireless System_Design, Performance, and Field Trial Results", *IEEE Communications Magazine*, vol. 40, no. 9, pp. 143-149, Sep. 2002.

[2] N. Thomos, N. V. Boulgouris, M.G. Strintzis, "Optimized Transmission of JPEG2000 Streams Over Wireless Channels", *IEEE Transactions on Image Processing*, vol. 15, no. 1, pp. 54-67, Jan. 2006.

[3] M. Agueh, J.-F. Diouris, M. Diop, F.-O. Devaux, C. De Vleeschouwer, B. Macq, "Optimal JPWL Forward Error Correction Rate Allocation for Robust JPEG 2000 Images and Video Streaming over Mobile Ad Hoc Networks", *EURASIP Journal on Advances in Signal Processing*, May 2008.

[4] M. F. Sabir, R. W. Heath, Jr., A. C. Bovik, "An Unequal Error Protection for Multiple Input Multiple Output Systems", *in Proceedings Record of the 36th Asilomar Conference on Signal, Systems and Computers.*, vol. 1, pp. 575-579, Nov. 2002.

[5] L. Atzori, "Transmission of JPEG2000 Images over Wireless Channels with Unequal Power Distribution", *IEEE Transactions on Consumer Electronics*, vol. 49, no. 11, pp. 883-888, Nov. 2003.

[6] M. El-Tarhuni, M. Assan, A. Bin Sediq, "A Joint Power Allocation and Adaptive Channel Coding Scheme for Image Transmission over Wireless Channels", *Journal of Computer Networks and Communications (IJCNC)*, vol. 2, no. 3, May 2010.

[7] M. F. Sabir, A.C. Bovik, R. W. Heath, Jr., "Unequal Power Allocation for JPEG Transmission Over MIMO Systems", *IEEE Transctions on Image Processing*, vol. 19, no. 2, pp. 410-421, Feb. 2010.

[8] A. Stanley, Y. Sun, "Space-time coding for Wireless communications: an overview", *IEEE Proceedings Communications*, vol. 153, no. 4, pp. 509-518, Aug. 2006.

[9] W. Hamidouche, C. Perrine, Y. Pousset, C. Olivier, "A solution to efficient power allocation for H.264/SVC video transmission over a realistic MIMO channel using precoder designs", *Journal of Visual Communication and Image Representation*, vol. 22, no. 6, pp. 563-574, Aug. 2011.

[10] P. J. Smith, L. M. Garth, M. Shafi, "Performance Analysis of Multiple-Input Multiple-Output Singular Value Decomposition Transceivers During Fading and Other Cell Interference", *IET Microwaves, Antennas & Propagation*, vol. 1, no. 6, pp. 1111-1119, 2007.

[11] H. Sampath, P. Stoica, A. Paulraj, "Generalized Linear Precoder and Decoder Design for MIMO Channels Using the Weighted MMSE criterion", *IEEE Transactions on Communications*, vol. 49, no. 12, pp. 2198-2206, Dec. 2001.

[12] P. Rostaing, O. Berder, L. Collin, G. Burel, "Minimum BER Diagonal Precoder for MIMO Digital Transmissions", *Signal Processing*, vol. 82, no. 10, pp. 1477-1480, 2002.

[13] L. Collin, O. Berder, P. Rostaing, G. Burel, "Optimal minimum distance-based precoder for MIMO spatial multiplexing systems", *in IEEE Transactions on Signal Processing*, vol. 52, no. 3, pp. 617-627, 2004.

[14] J. Abot, C. Olivier, C. Perrine, Y. Pousset, "A Link Adaptation Scheme Optimized for Wireless JPEG 2000 Transmission over Realistic MIMO Systems", *in Signal Processing: Image Communication*, vol. 27, no. 10, pp. 1066-1078, Nov. 2012.

[15] ISO/IEC 15444-11:2007, "JPEG 2000 Image Coding System – part11: Wireless JPEG 2000", May 2007.

[16] J. Abot, M. Nauge, C. Perrine, M.-C. Larabi, C. Bergeron, C. Olivier, Y. Pousset, "A Robust Content-Based JPWL Transmission Over a Realistic MIMO Channel Under Perceptual Constraints", *International Conference on Image Processing (ICIP'11)*, pp. 3241-3244, Brussels, Belgium, Sep. 2011.

[17] Y. Chartois, Y. Pousset, R. Vauzelle, "A SISO and MIMO Radio Channel Characterization with a 3D Ray Tracing Propagation in Urban Environment", *European Conference on Propagation and Systems*, Mar. 2005.

[18] A. Goldsmith, "Wireless Communications", Cambridge University Press, 2005.

[19] IEEE Standard for Information Technology-Part11: Wireless LAN Medium Access Control (MAC) and Physical Layer (PHY) Specifications Amendment: Enhancements for Higher Throughput (802.11n), 2009.

[20] V. Tarokh, A. Naguib, N. Seshadri, A. R. Calderbank. Space-time code for high data rate wireless communication: "Performance criteria in the presence of channel estimation errors, mobility, and multiple paths", *IEEE Transactions on Communications*, vol. 47, no. 2, Feb. 1999.